Published in final edited form as:

J Leukoc Biol. 2018 August ; 104(2): 239–251. doi:10.1002/JLB.3HI1217-488R.

Elevated nuclear lamin A is permissive for granulocyte transendothelial migration but not for motility through collagen I barriers

Sandeep Kumar Yadav[*], **Sara W. Feigelson**[*], **Francesco Roncato**[*], **Merav Antman-Passig**[§], **Orit Shefi**[§], **Jan Lammerding**[†], and **Ronen Alon**[*,¶]

[*]Department of Immunology, The Weizmann Institute of Science, Rehovot, Israel, 76100

[§]Faculty of Engineering, Bar Ilan Institute of Nanotechnologies and Advanced Materials, Bar Ilan University, Ramat Gan, Israel

[†]Nancy E. and Peter C. Meinig School of Biomedical Engineering, Weill Institute for Cell and Molecular Biology, Cornell University, Ithaca, New York

Abstract

Transendothelial migration (TEM) of lymphocytes and neutrophils is associated with the ability of their deformable nuclei to displace endothelial cytoskeletal barriers. Lamin A is a key intermediate filament component of the nuclear lamina which is downregulated during granulopoiesis. When elevated, lamin A restricts nuclear squeezing through rigid confinements. To determine if the low lamin A expression by leukocyte nuclei is critical for their exceptional squeezing ability through endothelial barriers, we overexpressed this protein in granulocyte-like differentiated HL-60 cells. A 10-fold higher lamin A expression did not interfere with chemokinetic motility of these granulocytes on immobilized CXCL1. Furthermore, these lamin A high leukocytes exhibited normal chemotaxis towards CXCL1 determined in large pore transwell barriers, but poorly squeezed through 3-μm pores towards identical CXCL1 gradients. Strikingly, however, these leukocytes successfully completed paracellular TEM across inflamed endothelial monolayers under shear flow, albeit with a small delay in nuclear squeezing into their sub-endothelial pseudopodia. In contrast, CXCR2 mediated granulocyte motility through collagen I barriers was dramatically delayed by lamin A overexpression due to a failure of lamin A high nuclei to translocate into the pseudopodia of the granulocytes. Collectively our data predict that leukocytes maintain a low lamin A content in their nuclear lamina in order to optimize squeezing through extracellular collagen barriers but can tolerate high lamin A content when crossing the highly adaptable barriers presented by the endothelial cytoskeleton.

[¶]Address correspondence to: Ronen Alon, Ph.D., Department of Immunology, The Weizmann Institute of Science, Rehovot, 76100, Israel. Tel: 972-8-9342482 Fax: 972-8-9344141 ronen.alon@weizmann.ac.il.

Conflict of Interest Disclosure

The authors declare no conflict of interest.

Authorship

S.K.Y. performed most of the experiments, analyzed data, and assisted in manuscript preparation and writing; S.W.F. assisted in FACS analyses and manuscript writing; F.R. performed some of the real time fluorescence microscopy experiments. JL provided reagents, expertise, and assisted in the interpretation of results and editing of the manuscript. R.A. designed and supervised experiments and wrote the manuscript.

Summary sentence:

Differential effects of nuclear stiffness on chemokine-driven leukocyte squeezing through endothelial and extracellular collagenous barriers

Introduction

The nucleus is the largest cellular organelle and is mechanically stabilized by a constitutive network of laminar proteins [1]. Nucleus deformation is the rate-limiting step for cells to pass through constrictions that are smaller than the nucleus size [1–5]. The mechanical stability of the nucleus, particularly for large deformations, is dictated by lamins, intermediate filaments proteins that form a network underlying the inner nuclear membrane [4, 6, 7]. Lamin A and its spliced variant lamin C impart the nucleus with its mechanical stability whereas the lamin B1 and B2 intermediate filaments are ubiquitously expressed but appear to be less important in mechanical stability of nuclei [8]. The nuclei of both circulating T-cells and neutrophils are soft due to a low content of lamin A/C and B in their lamina [9]. Furthermore, in contrast to epithelial and mesenchymal cells and solid tumors, which usually keep their stiff nuclei at their rear, motile leukocytes translocate their soft nucleus to their leading edge (pseudopodia) irrespective of the barriers they cross [10]. However, the relationship between lamin composition, nuclear stiffness and nucleus location and the impact of each of these parameters on the squeezing ability of leukocytes and other cells remains obscure.

It has been traditionally argued that leukocyte squeezing through endothelial barriers and extracellular barriers composed of collagen fibers involves passage through sub-micron wide gaps. Recent reports suggest, however, that leukocyte TEM involves a considerable widening of paracellular endothelial junctions as well as transcellular endothelial channels by the squeezing leukocyte [10, 11]. This leukocyte driven widening involves large displacement of endothelial stress fibers rather than active endothelial contractility [10, 11]. Our real-time imaging of nuclei in transmigrating leukocytes also suggested that the endothelial gap widening by squeezing leukocytes is driven by nuclear lobes, which are either preexistent or de novo formed by the deformable nuclei of T-cells [10]. This recent analysis of nuclear squeezing dynamics also raised the possibility that nuclear deformation determines both the gap size generated by squeezing leukocytes during TEM and the dynamics of nuclear squeezing [10]. Leukocyte nuclei appear to function as mechanical “drillers” that displace and collapse different actin assemblies within the endothelial cytoskeleton [10]. Nevertheless, a direct molecular demonstration that nuclear deformation and mechanical stiffness determine leukocyte passage through endothelial barriers and control gap sizes has been missing.

To address these standing questions, we have used a model system based on differentiated HL-60, human promyelocytic leukemia cells, which upon in vitro differentiation give rise to either granulocyte-like leukocytes or macrophages [12]. Whereas genetic manipulation of freshly isolated neutrophils is difficult and can result in side effects caused by the procedures required for ectopic gene expression, HL-60 cells can be readily transfected or transduced with target vectors prior to their differentiation into short-lived granulocyte-like cells. This

line has therefore been widely used for structural and functional assays of leukocytes [12–15]. Forced expression of lamin A in a similar HL-60 system, differentiated using all-trans-retinoic acid (ATRA) stimulation for 5 days, impaired nuclear lobulation during differentiation and inhibited serum triggered leukocyte perfusion through narrow channels and migration through rigid pores [16]. We used a similar system of DMSO differentiated HL-60 to generate granulocyte-like cells with 10-fold higher expression of lamin A. Having validated that the ability of these cells to transit through rigid micron-scale constrictions is severely compromised, we further investigated the ability of these leukocytes to squeeze through inflamed endothelial monolayers as well as through distinct fibrous barriers. Our results indicate that granulocytes overexpressing lamin A successfully adhered to and squeezed through confluent inflamed endothelial cell monolayers and successfully completed TEM in response to chemotactic signals, displacing the endothelial cytoskeleton and translocating their body underneath the monolayer, albeit with slightly delayed rates and creating larger pores in the endothelial layer. On the other hand, these lamin A enriched cells exhibited major defects in their ability to migrate through collagen I barriers in response to similar chemotactic signals. Our results suggest that chemokine-guided leukocyte squeezing through different cytoskeletal and extracellular matrix barriers is restricted to different extents by a given alteration in the stiffness of the leukocyte nuclear lamina.

Materials and Methods

Reagents and antibodies

Human CXCL1 was purchased from Peprotech (Rocky Hill, NJ, USA). PE-anti-human CD11a, PE-anti-human/mouse CD11b (M1/70), PE-anti-human CD29 and PE-anti-human CXCR2 antibodies were purchased from Ebioscience-Thermo Fisher Scientific (Waltham, MA, USA). HECA-452 was purchased from BD Bioscience Pharmingen (Franklin Lakes, New Jersey, USA). Anti CD18 mAb (TS1/18) was a kind gift from D. Staunton (ICOS, Bothell, WA, USA). Anti lamin A/C mAb was purchased from Santa Cruz Biotechnology (Dallas, Texas, USA). Rabbit polyclonal anti-human Lamin B1 was a kind gift from E. Gomes (University of Lisbon). Alexa 647 anti VE-cadherin mAb was purchased from Biolegend (San Diego, CA). R-Phycoerythrin AffiniPure F(ab')2 Fragment Goat Anti-Rat IgM (μ chain specific) and Goat Anti-Mouse IgG (H+L) antibodies were purchased from Jackson ImmunoResearch Laboratories, INC. (West Grove, PA, USA). Bovine Serum Albumin (BSA; fraction V), Hoechst, HEPES, CaCl2, MgCl2, and Hank's Balanced Salt Solution (HBSS) were purchased from Sigma-Aldrich (St. Louis, MO, USA).

Cell culture

The CXCR2-HL-60 cell variant line was described elsewhere [17]. Both parental HL-60 [16 1531] and the CXCR2-HL-60 variants were grown in RPMI-1640 medium supplemented with 20mM HEPES, 10% fetal calf serum, L-glutamine and Pen-Strep-Amphotericin. Cells were maintained at less than 1×10^6 cells/ml and differentiated into granulocyte-like cells (dHL-60) by culturing for 7 days in culture medium supplemented with 1.3% (V/V) Dimethyl Sulfoxide (DMSO). Granulocyte-like appearance was confirmed by upregulation of CD11a and CD11b (Suppl. Fig. 1A, B). HDMVECs (C-12211; PromoCell, Heidelberg,

Germany) were grown in PromoCell EC medium MV (C-22020), according to manufacturer's protocol and were used at passages 2–3.

Retroviral transduction

Stably modified lamin A overexpressing (LaminA-OE) CXCR2-HL-60 cells were generated by retroviral transduction with a bicistronic vector pRetroX-PrelaminA-IRES-ZsGreen1 as described [16]. A ZsGreen1 retroviral vector was used to generate the mock control cells. Retroviruses were produced by transfecting Phoenix cells using Lipofectamine® 2000 reagent following manufacturer's protocol. Retrovirus containing supernatant was collected at 48 hrs post transfection and used fresh to infect CXCR2-HL-60 cells in the presence of 4 mg/ml polybrene (Sigma). Cells were either sorted and maintained at >90% purity or taken as a mixture of lamin A-ZsGreen1 expressing and non-expressing cells for differentiation into granulocyte like cells using DMSO.

Flow Cytometry

For analysis of integrin or chemokine surface expression, cells were incubated with primary fluorescence-labeled mAb (CD11a, CD29, CD11 b: 10 Mg/ml) or unlabeled mAb (CXCR2, CD18, HECA-452: 10 ug/ml) followed by secondary antibodies (1:100, Jackson Immunoresearch) for 20 min at 4°C per incubation. For intracellular stainings, cells were fixed in chilled 80% methanol for 5 min, followed by 3 washes and permeabilization with tween (0.1%, PBS, 20 min at RT). Cells were incubated with anti-CD16/CD32 (10 μg/ml diluted in 10% goat serum) for 20 min RT for blockage of Fc receptors. Cells were then incubated with primary antibody (αLamin A/C or mIgG isotype control) diluted in 10% goat serum for 30 min at RT, washed, and stained with phycoerythrin-labeled goat anti-mouse secondary antibodies (1:100) for 30 min at RT in the dark. Antibody stainings and washes were carried out in fluorescence-activated cell sorting (FACS) buffer (Ca^{2+} and Mg^{2+} free PBS (PBS−/−), 1% BSA, 5mM EDTA, and 0.01% sodium azide). Stained cell suspensions were washed and resuspended in PBS+/+ prior to analysis by CytoFlex flow cytometer (Beckman Coulter). Data were acquired with CytExpert software (Beckman Coulter) and post-acquisition analysis was performed using FlowJo software (Tree Star, Inc.).

Cell proliferation assay

250,000 cells/ml were plated (Day 0) in a 10 cm culture plate. Cell count was determined every 24 hours over the course of four days by forward and side scattering and by ZsGreen1 fluorescence in a Cytoflex Flow Cytometer (Beckman Coulter Life Sciences, USA).

Analysis of leukocyte migration under shear flow

Primary HDMVECs were plated at confluence on either plastic or glass bottom 60 mm petri dishes coated with 2 μg/ml fibronectin (cat. # F0895; Sigma Aldrich, USA). A day later, cells were stimulated for 3 hrs. with IL-β (2 ng/ml). Endothelial cell coated plates were assembled in a flow chamber and washed extensively with the binding medium HBSS (Hank's balanced-salt solution containing 2 mg/mL BSA and 10 mM HEPES, pH 7.4, supplemented with 1 mM $CaCl_2$ and 1 mM $MgCl_2$). Neutrophil-like cells were perfused over the monolayer in binding medium for 40 s at 1.5 dyn/cm^2, and were then subjected to a

shear stress of 5 dyn/cm^2 for 10 min. Images were acquired at an interval of 15 sec using IX83, Olympus microscope equipped with 20× or 60× phase contrast objectives. Cells were tracked individually using ImageJ and categorized in at least 3 fields of view (~50 cells per field) as previously described [18, 19].

For analysis of migratory categories, leukocytes accumulated during the accumulation phase (40 seconds) were individually tracked throughout the assay by time-lapse microscopy and categorized as fractions of leukocytes originally accumulated at the end of this accumulation phase. Crawling leukocytes were defined as cells moving a distance of at least 30 Mm from their initial point of arrest. Transmigrating leukocytes were defined as either arrested or crawling cells which translocated their entire body through the endothelial monolayer. To monitor nuclear translocation and shape changes during TEM, cells were labelled with Hoechst 33342 as described [10] shortly before their introduction into the flow chamber. The location of pseudopodia sent by individual transmigrating dHL-60 cells and their respective nuclei were manually determined from time-lapse recordings (images were captures at 15 sec intervals). Gap size generated by transmigrating Hoechst labeled dHL-60 cells was determined as described by the displacement of a non blocking Alexa 647 anti-VE- cadherin mAb [10] (incubated at 2 μg/ml, 10 min prior to the beginning of the TEM assay). Since the majority of the gaps were oval, an average of both the long and short axes was calculated for each gap generated by transmigrating granulocyte-like dHL-60 cells.

Transwell migration assay

Differentiated HL-60 cells were washed with PBS (−/−) containing 5 mM EDTA, resuspended at a density of 2×10^6 cells/ml in binding medium HBSS (described above), and seeded in the upper chamber of 24-well transwells with 3 or 5-μm pore sizes (BD Biosciences, San Jose, CA, USA). The bottom chambers were filled with the corresponding media supplemented with and without CXCL1 (50 ng/ml) and incubated at 37°C in 5% CO_2 for 30 min. The transwell inserts were removed, the cells recovered from the bottom chambers were collected, and their numbers were determined by FACS analysis using the CytoFlex flow cytometer (Beckman Coulter).

Nuclear shape analysis and location

Hoechst 33342 labelled granulocyte-like HL-60 cells were allowed to settle for 15 min at 37°C on poly-L-Lysine (PLL) coated glass surface prepared by incubating PLL (0.01% w/v in ddH_2O) for 30 min at 37°C. Images were acquired using a 20× objective (IX83, Olympus, Shinjuku, Tokyo, Japan). Nuclear circularity index was determined using ImageJ. Similarly, nuclear circularity index was determined for Hoechst labeled granulocyte like HL-60 cells migrating over immobilized CXCL1. Thirty consecutive frames were captured for each granulocyte at 15 sec intervals, and the circularity index values in each frame were averaged for each cell. Nuclear location in each of these cells was manually determined. The nuclear locations of polarized and motile granulocytes were classified manually using CellSens Dimension Desktop software (Olympus) as either anterior and posterior based on whether the nuclei remained confined to either the leading or trailing edges, respectively for at least half of the total assay period.

Chemokine mediated 2D and 3D cell motility assays

Ibidi chamber slides (μ-Slide VI 0.4, Ibidi) were coated with 50 ng/ml CXCL1. Granulocyte-like dHL-60 cells were washed and resuspended in binding solution, injected into the Ibidi chamber and allowed to settle for 10 min at 37°C, and images were acquired with a 20× or 60× objective (IX83, Olympus). Velocity calculations were performed using ImageJ and trajectory analysis was performed using Imaris 9.0.0 (Bitplane, Belfast, UK) software. For 3D migration assays, granulocyte-like dHL-60 cells were washed and resuspended in cold matrigel solution (BD-356234, stock solution mixed with binding medium at 1:1 ratio) or in cold collagen I solution (rat tail, Corning, 3.2 mg/ml in binding medium) and injected into the Ibidi chamber at 4°C. The cells were sedimented at 50×g for 3 minutes and incubated under the matrigel or collagen I solutions at 37°C for 30 min to allow collagen polymerization. Images were acquired with a 20× or 60× objective (IX83, Olympus) for 30 min at intervals of 60 sec. Nuclear location and granulocyte velocities were determined with ImageJ software.

Confocal reflectance microscopy

Collagen I and matrigel solutions were prepared as described above, plated in 35-mm petri dishes and incubated for 30 minutes at 37°C in a humidified incubator. Gels were imaged using a Leica TCS SP5 confocal microscope by a 63×, 0.9 NA water immersion lens. Samples were illuminated with 488 nm Argon laser light and the meta channel of the microscope was set to detect wavelengths between 474 and 494 nm to allow reflectance mode [20].

Scanning electron microscopy of collagen matrices

Samples were fixed using 2.4% paraformaldehyde/2.5% glutaraldehyde in 0.1 M sodium cacodylate buffer for 1 hr at RT. After fixation, samples were rinsed repeatedly with PBS−/− (without Ca^{2+} or Mg^{2+}, pH 7.4) and then treated with guanidine-HCl/tannic acid (4:5) solution (2%) for 1 hr. at RT. Samples were rinsed repeatedly with PBS−/− and then dehydrated in a graded series of 50%, 70%, 80%, 90% and 100% ethanol/water (v/v) for 10 minutes each. The residual ethanol was then removed using a series of 50%, 75% and 100% (x3) Freon solutions in ethanol for 10 min each. Finally, the samples were air dried for few seconds. The dried samples were mounted on aluminum stubs, sputter coated with carbon and, viewed with the SEM (FEI Quanta 250 FEG, OR, USA).

Statistical Analysis

All the data are reported as the sample mean ± SD or SEM, as indicated, and means of different groups were compared pairwise using two-tailed, unpaired student’s t-test. The difference between two datasets was considered significant for p values below 0.05.

Results

Lamin A overexpression in granulocyte-like cells does not affect their chemokinesis but restricts migration through small, rigid pores

Primary neutrophils as well as granulocyte-like differentiated HL-60 cells (dHL-60) downregulate expression of the nuclear lamina proteins lamin A and C during differentiation [9]. In our experiments, we used a variant of HL-60 that stably expresses CXCR2 levels comparable to those in primary neutrophils [21] in order to facilitate migration of these leukocytes across CXCL1-producing inflamed endothelial cell monolayers. This introduced CXCR2 expression was critical for the ability of these cells to cross IL-1β-stimulated HDMVEC, a well-studied low permeability endothelial barrier, which supports robust neutrophil accumulation and TEM under physiological shear flow [10, 19] (Figure 1A and data not shown). To overexpress lamin A in these HL-60 variants, we infected them with an IRES containing retroviral vector co-encoding the pre lamin A precursor and a ZsGreen1 reporter as previously described [16]. ZsGreen1 expressing cells were found to have 10-fold higher levels of lamin A than control CXCR2-HL-60 cells, when differentiated with DMSO into granulocyte-like cells (Figure 1B). Importantly, lamin A overexpression in these granulocyte-like leukocytes did not impair their proliferation rates, nor alter Lamin B1 expression, CXCR2 levels or change the levels of major integrin members or the expression of E-selectin carbohydrate ligands (Figure 1C–H and Suppl. Fig. 1C, D). Lamin A overexpression also did not affect chemokinetic motility of the differentiated granulocyte-like CXCR2-HL-60 cells (henceforth referred to as CXCR2-dHL-60) measured on a 2D surface coated with the CXCR2 chemokine CXCL1 (Figure 1I). The lamin A overexpressing granulocyte-like dHL-60 cells also normally crossed through 5 μm pore transwells towards a CXCL1 gradient, comparable to non-modified control cells (Figure 2A). However, when compared for their ability to squeeze towards identical CXCL1 gradients through transwells containing 3 μm pores, which are substantially smaller than their nuclear diameter, only a minute fraction of laminA-OE CXCR2-dHL-60 successfully passed through these smaller pores, whereas control CXCR2-dHL-60 cells showed efficient migration through these pores, albeit less than in the larger pores (Figure 2A). Notably, lamin A overexpression did not change the nuclear shape of these differentiated HL-60 cells as assessed by the average circularity of the nuclei in these granulocyte-like cells settled on a poly-L-lysine substrate (Figure 2B,C). Given that lamin A overexpression had only a moderate or no effect on nuclear circularity (Figure 2B–D), we conclude that the impaired migration of lamin A overexpressing CXCR2-dHL-60 cells through 3- um pores is caused by the increased nuclear stiffness due to higher lamin levels, and not an increase in nuclear circularity. These migration results are consistent with previous findings in dHL-60 granulocyte-like cells obtained by ATRA treatment [16].

To further validate that the ZsGreen1 reporter on its own is inert in our various assays, the ZsGreen1 gene alone was introduced into CXCR2-dHL-60 cells by an identical viral vector, and both ZsGreen1 expressing and nonexpressing CXCR2-dHL-60 cells were compared for their ability to cross rigid transwell pores and transmigrate across inflamed endothelial barriers. As expected, the ZsGreen1 expressing granulocyte-like CXCR2-dHL-60 normally crossed through small rigid pores towards CXCL1 gradients (Supplemental Figure 1E).

Thus, high-level expression of the ZsGreen1 reporter, on its own, does not alter the mechanical properties and squeezing capacity of CXCR2-dHL-60 cells. This observation also suggested that the ZsGreen1 negative granulocyte-like CXCR2-dHL-60 cells are practically identical to ZsGreen1 expressing granulocyte-like CXCR2-dHL-60 cells with respect to their mechanical nuclear properties. Hence, in all the rest of the experiments we assessed the motility and squeezing of the granulocyte-like CXCR2-dHL-60 cells co-expressing high ZsGreen1 and high lamin A levels to those of similarly co-cultured and co-differentiated granulocyte-like CXCR2-dHL-60 cells which did not overexpress lamin A.

Lamin A overexpression in granulocyte-like cells is permissive for protrusion and TEM but slows down nuclear squeezing through endothelial junctions

To further elucidate the effect of lamin A overexpression on dHL-60 migration across endothelial barriers, we next determined the adhesive and migratory capacities of ZsGreen1-LaminA overexpressing granulocyte-like CXCR2-dHL-60 (green cells) to CXCR2-dHL-60 cells which did not express the ZsGreen1-lamin A construct. When both populations were perfused under shear flow on low permeability confluent monolayers of HDMVECs stimulated by IL-β [10], lamin A overexpressing dHL-60 cells normally resisted detachment by continuously applied shear forces (Figure 3A). Both groups of dHL-60 cells arrested nearby the endothelial junctions they eventually transmigrated through while exhibiting negligible lateral crawling on the apical endothelial surfaces (Figure 3A). Surprisingly, although lamin A overexpressing granulocyte-like dHL-60 cells failed to squeeze through 3-μm diameter rigid pores (Figure 2B), comparable fractions of lamin A overexpressing and control CXCR2-dHL-60 transmigrated through IL-1β inflamed HDMVECs (Figure 3A, TEM category). Nevertheless, kinetic analysis of the TEM of these leukocytes revealed a statistically significant delay of the lamin A overexpressing cells compared to the control cells (Figure 3B,C). In order to further elucidate at a single cell level the basis for this delay in successful TEM, we analyzed the kinetics of leukocyte protrusion through the endothelial monolayer, as well as the overall time spent by either individual control or high lamin A expressing dHL-60 cells subsequent to this initial protrusion underneath the endothelial monolayer until the completion of TEM. While the rate of protrusion and extension of a basolateral pseudopodium (leading edge) underneath the endothelial monolayer was indistinguishable between control and lamin A overexpressing CXCR2-dHL-60 cells (Figure 3D,E), the lamin A overexpressing CXCR2-dHL-60 cells had an over 30% increase in the average period required for TEM completion compared with control CXCR2-dHL-60 cells (Figure 3F). Notably, the periods required for TEM completion of individual granulocytes was highly variable for both lamin A low and high CXCR2-dHL-60 cells, reflecting the multiple barriers these leukocytes had to overcome to successfully cross the inflamed endothelial monolayers.

Further comparison of Hoechst labeled control and lamin A high CXCR2-dHL-60 cells indicated that the main step delayed for the lamin A overexpressing CXCR2-dHL-60 cells was the time it took the nuclei of these cells to completely pass through the endothelial barrier (Figure 4A,B and Video 1). In contrast, the rate of retraction of the uropod of these cells was comparable (data not shown). These results collectively suggest that the nuclei of granulocytes overexpressing lamin A are delayed in their insertion into the otherwise normal

basolateral pseudopodia generated by these granulocytes in response to chemotactic CXCR2 signals. Thus, their ability to lift the endothelial cells engaged by their basolateral pseudopodia and open gaps between neighboring endothelial cells is impaired, resulting in considerably larger subendothelial pseudopodia (Figure 4A and Video 1).

We have recently shown that leukocyte nuclear squeezing through transcellular routes of TEM is associated with pore widening to about 5 μm in diameter [10]. We therefore asked if granulocyte-like cells that overexpress lamin A and are delayed in their squeezing through endothelial gaps exceed this upper limit of endothelial gaps. To address this question, we probed gap formation by VE-cadherin displacement by our different granulocyte-like CXCR2-dHL-60 cells. Remarkably, the average gap size generated by lamin A overexpressing CXCR2-dHl-60 cells was 20% larger than the average gap diameter generated by control CXCR2-dHL-60 cells (Figure 4C) consistent with the higher circularity of the nuclei of lamin A overexpressing CXCR2-dHL-60 cells polarized on immobilized CXCL1 (Figure 2D). These larger openings created in the endothelial layer may explain why lamin A overexpressing CXCR2-dHL-60 cells have similar TEM efficiency as control cells, despite their rounder and less deformable nuclei. Notably, both lamin A overexpressing and control CXCR2-dHL-60 cells readily displaced the stress fibers of the individual endothelial cells they squeezed between, without rupturing these fibers (data not shown).

Lamin A overexpression in granulocyte-like cells restricts chemokine driven motility through and crossing of collagen I barriers

Extravasating leukocytes must cross additional extracellular matrix barriers upon exiting blood vessels and crossing the basement membrane deposited by both the endothelial cells and their neighboring pericytes [22]. To mimic the barriers encountered by leukocytes during interstitial motility, we designed a new readout, which combines chemokine driven leukocyte motility on a rigid 2D surface with a mechanical barrier exerted by a 3D matrix composed of distinct collagen containing fibrous barriers. To this end, both lamin A overexpressing and control CXCR2-dHL-60 cells were settled on a glass slide coated with CXCL1 in the presence of medium alone or medium supplemented with either 50% matrigel, which was allowed to undergo in situ polymerization for 20–30 min at 37°C, or medium supplemented with collagen I allowed to undergo identical in situ polymerization (Figure 5A). Matrigel is an extract derived from mice harboring tumors, and is rich in laminin and collagen IV and is therefore sometimes used as a surrogate basement membrane [23]. While both collagen I and matrigel are commonly used models of cell invasion, they have distinct biomechanical properties. Matrigel is characterized by small pore sizes and high deformability, while collagen I matrices at comparable collagen concentrations have larger pore sizes but are less deformable [23]. Comparison of these two types of barriers using confocal reflective microscopy revealed that the collagen I barrier is composed of thick fibers as opposed to the matrigel (Figure 5B). SEM analysis of these matrices [24] further supported the notion that the collagen I matrix is much denser than the matrigel matrix (Suppl. Fig. 2).

We next compared both the nucleus location and the motility of either control or lamin A overexpressing CXCR2-dHL-60 cells settled on CXCL1 in the presence of these different

media (Figure 6A–D). Notably, in aqueous media, dHL-60 with high lamin A content underwent normal polarization on CXCL1 coated 2D surfaces (Figure 6A, Video 2), the nuclei of both granulocytes were readily translocated into their leading edges (Figure 6C, and Video 2), and both granulocytes locomoted at comparable velocities on this 2D substrate (Figure 6D and Video 2). As expected, the granulocyte-like CXCR2-dHL-60 cells locomoted more slowly on immobilized CXCL1 when embedded inside the matrigel relative to when the same cells were settled on the immobilized CXCL1 in medium only (Figure 6B, D and Video 3). Nevertheless, in the presence of the matrigel, lamin A overexpression modestly affected nuclear translocation into the leading edge of migrating granulocytes (Figure 6C and Video 3) and reduced granulocyte motility by only ~20% (Figure 6D). These results indicate that the stiffer nuclei of lamin A overexpressing granulocyte-like CXCR2-dHL-60 cells only marginally restrict the 2D chemokinetic motility when the cells are embedded inside a soft matrigel barrier and do not restrict the nuclear translocation and motility of these cells in aqueous medium. Since none of the lamin A high granulocyte-like CXCR2-dHL-60 cells were arrested by the matrigel barrier, and the majority of their nuclei readily translocated into the leading edge of motile leukocytes (Figure 6B–D, Video 3), these results indicate that when the porous barrier is sufficiently deformable, most lamin A overexpressing, stiff leukocyte nuclei can override the low resistance imposed by such a barrier.

To evaluate the contrasting scenario of a less deformable extracellular matrix network, we assessed the impact of leukocyte nuclear stiffness on squeezing through a distinct porous barrier that closely resembles the collagen I rich interstitial tissue encountered by leukocytes once they enter peripheral tissues [25]. We therefore compared the ability of lamin A overexpressing and control CXCR2-dHL-60 cells settled on immobilized CXCL1 and embedded in a matrix of pure collagen I to cross this barrier. Notably, the vast majority of lamin A high granulocyte-like CXCR2-dHL-60 cells failed to translocate their nuclei to their protrusive leading edges in spite of their normal ability to extend filopodia-like protrusions (Figure 7A, B and Video 4). Consequently, lamin A overexpressing cells showed a substantially reduced motility when embedded in the collagen I matrix compared with control granulocyte-like CXCR2-dHL-60 cells (Figure 7C), and their ability to successfully move through the collagen, although inherently variable, was significantly impaired (Figure 7D). Interestingly, polymerized collagen I did not slow down the motility of normal granulocyte-like CXCR2 dHL-60 cells more than did the matrigel barrier (i.e. a mean velocity of ±6.1 in collagen I compared to a mean velocity of ±6.6 in matrigel), indicating that it imposed a major barrier selectively on the migration of lamin A overexpressing granulocyte-like cells, which have stiffer nuclei [16], whereas control ganulocyte-like cells with their highly deformable nuclei can still easily penetrate the collagen I matrix. The dramatically slower motility of these granulocytes through the collagen I gel and retarded nuclear translocation to the leading edge of these leukocytes was not the result, however, of augmented integrin mediated adhesiveness of the lamin A overexpressing CXCR2-dHL-60 cells to the collagen I fibers because the motility of these granulocytes was not affected by exclusion of Mg^{++} (data not shown). Thus, integrin-independent CXCR2 mediated granulocyte motility through collagen I barriers is dramatically delayed by lamin A

overexpression due to a failure of the stiffer, lamin A high nuclei to translocate into the pseudopodia of granulocytes crossing this poorly deformable barrier.

Discussion

The lamin cortex of all mammalian nuclei is a thin, elastic shell encoded by three functionally nonredundant genes, *LMNA,* encoding lam ins A/C, and *LMNB1* and *LMNB2,* encoding lamin B1 and lamin B2, respectively [26]. Lamins exist in dynamic equilibrium between the nucleoplasm and the lamina network [27]. The ratio between the *LMNA* gene products lamin A and its shorter spliced variant lamin C and the other lamins is proportionally related to nuclear stiffness in both mesenchymal and hematopoietic cells [28]. In addition to their roles in structure and nuclear stability, the various lamins are also involved in transcription, chromatin organization and DNA replication and their mutations are associated with multiple pathologies [29, 30]. Nevertheless, the lamin A overexpression in our model HL-60 cell system did not affect the expression of the canonical surface markers associated with this differentiation or of key functional receptors involved in leukocyte TEM and motility such as integrins and myeloid GPCRs. Furthermore, lamin A overexpression did not affect the migratory properties of dHL-60 cells under different conditions such as chemokine driven motility on 2D surfaces or chemotaxis through large rigid pores, suggesting that their differentiation and major cytoskeletal machineries were not functionally affected by lamin A overexpression.

Circulating leukocytes express very low lamin A levels, which keep their nuclei soft and thereby presumably allowing these cells to readily squeeze through vascular barriers [1]. Strikingly, however, our granulocyte-like cells genetically manipulated to express 10-fold higher levels of lamin A could still readily cross the low permeability endothelial barriers used in our in vitro TEM setups. These results suggest that leukocytes with stiff nuclei can open up sufficiently large gaps in between neighboring ECs, orders of magnitude larger than the gaps these cells normally maintain to squeeze their nuclei through these openings and lift these endothelial cells microns above the basement membrane they normally deposit [31]. Thus, while lamin A overexpressing cells take slightly longer to transmigrate through an endothelial cell monolayer, they eventually successfully transmigrate through this barrier, and this is accomplished by opening larger gaps in between neighboring endothelial cells that allow transit of the more rigid nuclei in the lamin A overexpressing cells.

Our data indicate that the size of endothelial gaps generated by squeezing leukocytes is probably dictated by the dimension of the leukocyte nuclei more than by the resistance of the endothelial cytoskeleton to leukocyte squeezing. The endothelial cells were traditionally proposed to facilitate gap enlargement via myosin driven contraction, yet we and other groups have recently ruled out this alternative mechanism for endothelial gap formation [10,11,32]. Our new results further suggest that endothelial gap formation is simultaneously regulated by both the leukocyte nuclei and by the endothelial cytoskeleton. In addition to restricting gap widening by squeezing leukocytes, the endothelial cytoskeleton restricts the ability of the endothelial cell to be lifted above the slide by the squeezed leukocyte nucleus. Our results indicate that even the dramatic stiffening introduced to the nuclear lamina of

granulocytes by lamin A overexpression only moderately affects this endothelial lifting, without which the leukocyte cannot complete its squeezing through endothelial monolayers.

The nuclear stiffening introduced by lamin A overexpression in our model granulocyte-like HL-60 cells exerted dramatic effects on the ability of these cells to squeeze and migrate through 3D collagen I matrices in response to chemokinetic CXCL1 signals. At the same time, lamin A high granulocytes successfully crossed the much softer matrigel barriers in response to identical chemokinetic CXCL1 signals. Notably, these cells also normally translocated their stiff nuclei to their lamellipodia and protrusions, further indicating that nucleus stiffening and lamin A overexpression, on their own, do not alter the position of the nucleus in migrating leukocytes. Rather, the translocation of the nucleus in motile leukocytes to the leukocyte lamellipodia is determined both by its relative stiffness and the relative mechanical resistance of the external environment surrounding the motile leukocyte. Why then did the same nuclear stiffening introduced by lamin A overexpression not affect granulocyte squeezing through matrigels? Whereas the components of matrigel are chemically similar to the major components of endothelial basement membranes, polymerized matrigel is mechanically softer than polymerized collagen I [33, 34]. Our structural analysis of 3D matrigel and 3D collagen I gels also indicates the presence of thick collagen fibers in the collagen I gels and absence in polymerized matrigels. This is attributed to the molecular differences between fiber-forming collagen I as opposed to the network assembly of collagen IV together with laminin within matrigels. The 3D collagen I barriers constructed by us in the present work appear to better mimic the physiologically relevant barrier leukocytes encounter during their interstitial motility in tissues. An open question of interest is the crossing ability of leukocytes with stiff nuclei through endothelial basement membrane barriers given that some basement membranes are discontinuous around post capillary venules at some sites of inflammation [35, 36].

One of the most surprising results of our study is the efficient squeezing of the lamin A high nuclei across endothelial junctions and underneath endothelial monolayers. This reflects the remarkable ability of the endothelial barrier to adapt its cytoskeleton to stiff lamin A high nuclei. This adaptive nature of the endothelial cytoskeleton sharply contrasts the mechanical resistance of collagen I fibers to the squeezing of identically stiff nuclei [37]. We thus predict, that unlike these fibers, both the endothelial actin filaments and microtubules that construct the main mechanical barriers of the endothelial cytoskeleton can likely bend, get displaced and undergo remodeling when crossed by either soft (i.e., lamin A low) or stiff (i.e., lamin A high) nuclei. The endothelial resistance to nuclear squeezing is low, likely because of the high elasticity of the endothelial stress fibers and the fast turnover of the short actin filaments interlaced in between these actin bundles [10, 32]. Our results also elude to the possibility that the pulling and pushing forces normally exerted by the leukocyte actomyosins are sufficiently high to propel even the stiffer nucleus of lamin A overexpressing leukocytes into the leukocyte pseudopodia and thereby override the low mechanical resistance imposed by the endothelial cytoskeleton. These actomyosin derived forces are also strong enough to squeeze the stiff lamin A enriched nuclei through thin and porous barriers such as those imposed by matrigels. Similar forces are, on the other hand, insufficient to override the indefinitely high mechanical resistance imposed on the same nuclei by rigid pores and by the high resistance imposed by stiff collagen I fibers.

In summary, our results highlight the permissive nature of the endothelial cytoskeleton, which is highly dynamic and can actively remodel and rapidly change its fine structure, compared to extracellular matrices, which are relatively passive materials. The remarkable adaptive nature of endothelial cytoskeletal barriers to nuclear squeezing warrants future in vivo analysis of the relative abilities of other leukocytes with variable content of nuclear lamin A and stiffness to squeeze through distinct vascular beds and their different basement membranes. Such future studies should provide additional insights as to why most leukocytes maintain a low lamin A content of their nuclei, while most other cells, including leukocyte precursors in the bone marrow and subsets of activated lymphocytes, benefit from high lamin A content of their nuclei [28, 38, 39].

Supplementary Material

Refer to Web version on PubMed Central for supplementary material.

Acknowledgements

We thank Dr. Ann Richmond (Vanderbilt University, Nashville, Tennessee) for providing the CXCR2 expressing HL-60 line. R.A. is the Incumbent of the Linda Jacobs Chair in Immune and Stem Cell Research. R.A. is supported by the Israel Science Foundation, the Flight Attendant Medical Research Institute Foundation (FAMRI), U.S.A., the Minerva Foundation, Germany as well as a research grant from Carol A. Milett. J.L. is supported by awards from the National Institutes of Health [R01 HL082792 and U54 CA210184], the Department of Defense Breast Cancer Research Program [Breakthrough Award BC150580], and the National Science Foundation [CAREER Award CBET-1254846 and MCB-1715606].

Abbreviations

dHL-60	differentiated HL-60 cells
EC	Endothelial Cells
HDMVEC	Human Dermal Micro-Vascular Endothelial Cells
HBSS	Hank’s Balanced Salt Solution
LBR	lamin B receptor
OE	Overexpressing
SEM	scanning electron microscopy
TEM	Transendothelial migration
2D	Two Dimensional
3D	Three Dimensional

References

1. Friedl P, Wolf K, Lammerding J (2011) Nuclear mechanics during cell migration. Curr Opin Cell Biol 23, 55–64. [PubMed: 21109415]
2. Khatau SB, Bloom RJ, Bajpai S, Razafsky D, Zang S, Giri A, Wu PH, Marchand J, Celedon A, Hale CM, Sun SX, Hodzic D, Wirtz D (2012) The distinct roles of the nucleus and nucleus- cytoskeleton connections in three-dimensional cell migration. Sci Rep 2, 488. [PubMed: 22761994]

3. Davidson PM, Denais C, Bakshi MC, Lammerding J (2014) Nuclear deformability constitutes a rate-limiting step during cell migration in 3-D environments. Cell Mol Bioeng 7, 293–306. [PubMed: 25436017]
4. Denais C and Lammerding J (2014) Nuclear mechanics in cancer. Adv Exp Med Biol 773, 435–70. [PubMed: 24563360]
5. Thiam HR, Vargas P, Carpi N, Crespo CL, Raab M, Terriac E, King MC, Jacobelli J, Alberts AS, Stradal T, Lennon-Dumenil AM, Piel M (2016) Perinuclear Arp2/3-driven actin polymerization enables nuclear deformation to facilitate cell migration through complex environments. Nat Commun 7, 10997. [PubMed: 26975831]
6. Fruleux A and Hawkins RJ (2016) Physical role for the nucleus in cell migration. J Phys Condens Matter 28, 363002. [PubMed: 27406341]
7. Stephens AD, Banigan EJ, Adam SA, Goldman RD, Marko JF (2017) Chromatin and lamin A determine two different mechanical response regimes of the cell nucleus. Mol Biol Cell 28, 1984–1996. [PubMed: 28057760]
8. Lammerding J, Fong LG, Ji JY, Reue K, Stewart CL, Young SG, Lee RT (2006) Lamins A and C but not lamin B1 regulate nuclear mechanics. J Biol Chem 281, 25768–80. [PubMed: 16825190]
9. Olins AL, Zwerger M, Herrmann H, Zentgraf H, Simon AJ, Monestier M, Olins DE (2008) The human granulocyte nucleus: Unusual nuclear envelope and heterochromatin composition. Eur J Cell Biol 87, 279–90. [PubMed: 18396345]
10. Barzilai S, Yadav SK, Morrell S, Roncato F, Klein E, Stoler-Barak L, Golani O, Feigelson SW, Zemel A, Nourshargh S, Alon R (2017) Leukocytes Breach Endothelial Barriers by Insertion of Nuclear Lobes and Disassembly of Endothelial Actin Filaments. Cell Rep 18, 685–699. [PubMed: 28099847]
11. Heemskerk N, Schimmel L, Oort C, van Rijssel J, Yin T, Ma B, van Unen J, Pitter B, Huveneers S, Goedhart J, Wu Y, Montanez E, Woodfin A, van Buul JD (2016) F-actin-rich contractile endothelial pores prevent vascular leakage during leukocyte diapedesis through local RhoA signalling. Nature Communications 7.
12. Collins SJ (1987) The HL-60 promyelocytic leukemia cell line: proliferation, differentiation, and cellular oncogene expression. Blood 70, 1233–44. [PubMed: 3311197]
13. Xu J, Wang F, Van Keymeulen A, Herzmark P, Straight A, Kelly K, Takuwa Y, Sugimoto N, Mitchison T, Bourne HR (2003) Divergent signals and cytoskeletal assemblies regulate self-organizing polarity in neutrophils. Cell 114, 201–14. [PubMed: 12887922]
14. Xu J, Wang F, Van Keymeulen A, Rentel M, Bourne HR (2005) Neutrophil microtubules suppress polarity and enhance directional migration. Proc Natl Acad Sci U S A 102, 6884–9. [PubMed: 15860582]
15. Gera N, Swanson KD, Jin T (2017) beta-Arrestin 1-dependent regulation of Rap2 is required for fMLP-stimulated chemotaxis in neutrophil-like HL-60 cells. J Leukoc Biol 101, 239–251. [PubMed: 27493245]
16. Rowat AC, Jaalouk DE, Zwerger M, Ung WL, Eydelnant IA, Olins DE, Olins AL, Herrmann H, Weitz DA, Lammerding J (2013) Nuclear envelope composition determines the ability of neutrophil-type cells to passage through micron-scale constrictions. J Biol Chem 288, 8610–8. [PubMed: 23355469]
17. Sai J, Walker G, Wikswo J, Richmond A (2006) The IL sequence in the LLKIL motif in CXCR2 is required for full ligand-induced activation of Erk, Akt, and chemotaxis in HL60 cells. J Biol Chem 281, 35931–41. [PubMed: 16990258]
18. Shulman Z and Alon R (2012) Real-time analysis of integrin-dependent transendothelial migration and integrin-independent interstitial motility of leukocytes. Methods Mol Biol 757, 31–45. [PubMed: 21909904]
19. Shulman Z, Cohen SJ, Roediger B, Kalchenko V, Jain R, Grabovsky V, Klein E, Shinder V, Stoler-Barak L, Feigelson SW, Meshel T, Nurmi SM, Goldstein I, Hartley O, Gahmberg CG, Etzioni A, Weninger W, Ben-Baruch A, Alon R (2012) Transendothelial migration of lymphocytes mediated by intraendothelial vesicle stores rather than by extracellular chemokine depots. Nat Immunol 13, 67–76.

20. Antman-Passig M, Levy S, Gartenberg C, Schori H, Shefi O (2017) Mechanically Oriented 3D Collagen Hydrogel for Directing Neurite Growth. Tissue Eng Part A 23, 403–414. [PubMed: 28437179]
21. Liu Y, Sai J, Richmond A, Wikswo JP (2008) Microfluidic switching system for analyzing chemotaxis responses of wortmannin-inhibited HL-60 cells. Biomed Microdevices 10, 499–507. [PubMed: 18205049]
22. Nourshargh S and Alon R (2014) Leukocyte migration into inflamed tissues. Immunity 41, 694–707. [PubMed: 25517612]
23. Sodek KL, Brown TJ, Ringuette MJ (2008) Collagen I but not Matrigel matrices provide an MMP-dependent barrier to ovarian cancer cell penetration. BMC Cancer 8, 223. [PubMed: 18681958]
24. Anguiano M, Castilla C, Maska M, Ederra C, Pelaez R, Morales X, Munoz-Arrieta G, Mujika M, Kozubek M, Munoz-Barrutia A, Rouzaut A, Arana S, Garcia-Aznar JM, Ortiz-de-Solorzano C (2017) Characterization of three-dimensional cancer cell migration in mixed collagen-Matrigel scaffolds using microfluidics and image analysis. PLoS One 12, e0171417. [PubMed: 28166248]
25. Sorokin L (2010) The impact of the extracellular matrix on inflammation. Nat Rev Immunol 10, 712–23. [PubMed: 20865019]
26. Funkhouser CM, Sknepnek R, Shimi T, Goldman AE, Goldman RD, Olvera de la Cruz, M. (2013) Mechanical model of blebbing in nuclear lamin meshworks. Proc Natl Acad Sci U S A 110, 3248–53. [PubMed: 23401537]
27. Pajerowski JD, Dahl KN, Zhong FL, Sammak PJ, Discher DE (2007) Physical plasticity of the nucleus in stem cell differentiation. Proc Natl Acad Sci U S A 104, 15619–24. [PubMed: 17893336]
28. Shin JW, Spinler KR, Swift J, Chasis JA, Mohandas N, Discher DE (2013) Lamins regulate cell trafficking and lineage maturation of adult human hematopoietic cells. Proc Natl Acad Sci U S A 110, 18892–7. [PubMed: 24191023]
29. Bell ES and Lammerding J (2016) Causes and consequences of nuclear envelope alterations in tumour progression. Eur J Cell Biol 95, 449–464. [PubMed: 27397692]
30. Tran JR, Chen H, Zheng X, Zheng Y (2016) Lamin in inflammation and aging. Curr Opin Cell Biol 40, 124–130. [PubMed: 27023494]
31. toler-Barak L, Barzilai S, Zauberman A, Alon R (2014) Transendothelial migration of effector T cells across inflamed endothelial barriers does not require heparan sulfate proteoglycans. Int Immunol 26, 315–24. [PubMed: 24402310]
32. Alon R and van Buul JD (2017) Leukocyte Breaching of Endothelial Barriers: The Actin Link. Trends Immunol 38, 606–615. [PubMed: 28559148]
33. Engbring JA and Kleinman HK (2003) The basement membrane matrix in malignancy. J Pathol 200, 465–70. [PubMed: 12845613]
34. Kalluri R (2003) Basement membranes: structure, assembly and role in tumour angiogenesis. Nat Rev Cancer 3, 422–33. [PubMed: 12778132]
35. Wang S, Voisin MB, Larbi KY, Dangerfield J, Scheiermann C, Tran M, Maxwell PH, Sorokin L, Nourshargh S (2006) Venular basement membranes contain specific matrix protein low expression regions that act as exit points for emigrating neutrophils. J Exp Med 203, 1519–32. [PubMed: 16754715]
36. Voisin MB, Probstl D, Nourshargh S (2010) Venular basement membranes ubiquitously express matrix protein low-expression regions: characterization in multiple tissues and remodeling during inflammation. Am J Pathol 176, 482–95. [PubMed: 20008148]
37. Yang YL and Kaufman LJ (2009) Rheology and confocal reflectance microscopy as probes of mechanical properties and structure during collagen and collagen/hyaluronan self-assembly. Biophys J 96, 1566–85. [PubMed: 19217873]
38. Gonzalez-Granado JM, Silvestre-Roig C, Rocha-Perugini V, Trigueros-Motos L, Cibrian D, Morlino G, Blanco-Berrocal M, Osorio FG, Freije JM, Lopez-Otin C, Sanchez-Madrid F, Andres V (2014) Nuclear envelope lamin-A couples actin dynamics with immunological synapse architecture and T cell activation. Sci Signal 7, ra37.
39. Rocha-Perugini V and Gonzalez-Granado JM (2014) Nuclear envelope lamin-A as a coordinator of T cell activation. Nucleus 5, 396–401. [PubMed: 25482193]

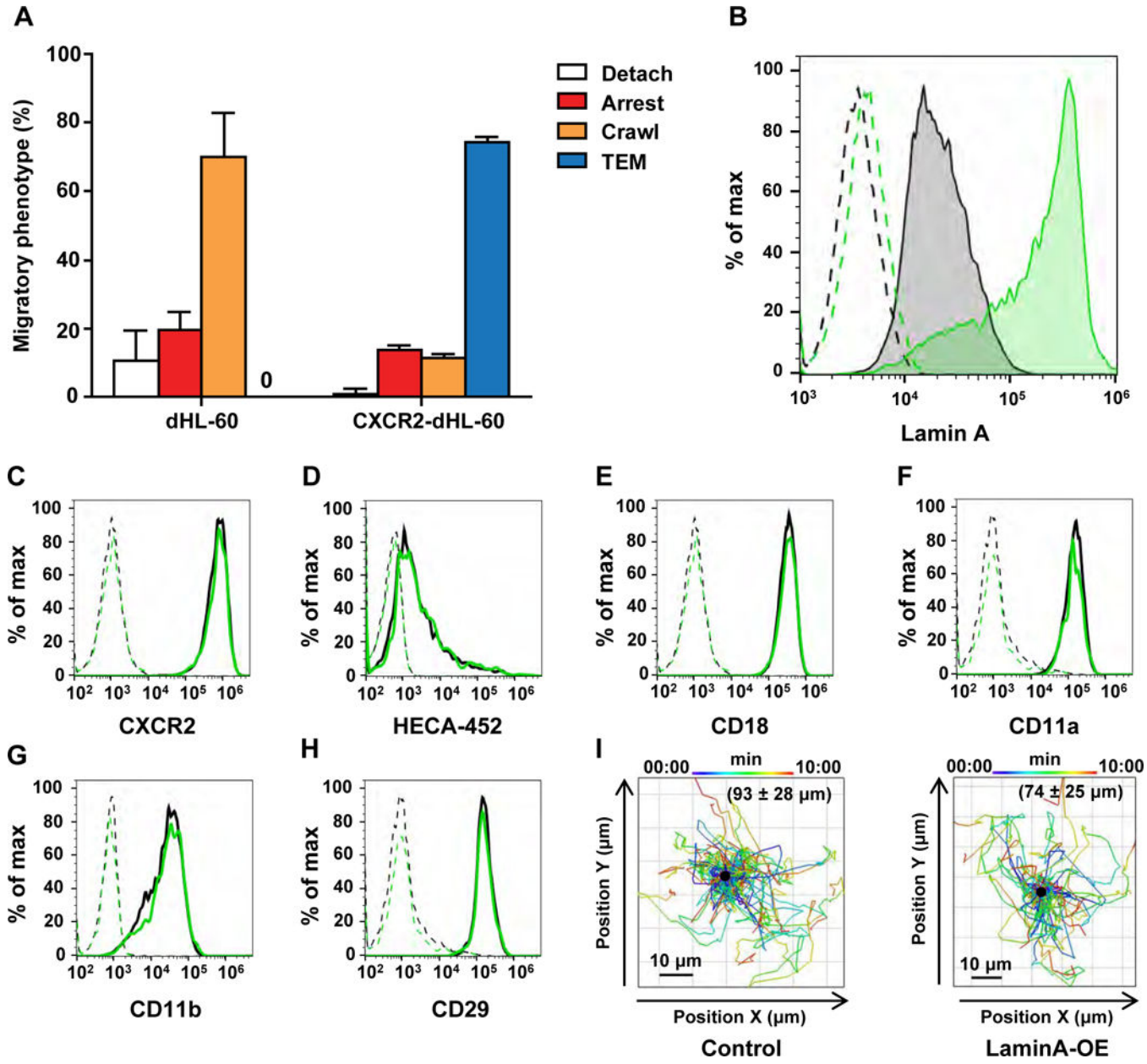

Figure 1. Lamin A overexpression in CXCR2 expressing granulocyte-like dHL-60 cells does not affect the surface expression of receptors involved in trans-endothelial migration and does not alter CXCL1 driven chemokinesis.

(A) Adhesive and migratory phenotypes of granulocyte-like DMSO differentiated HL-60 (dHL-60) variants deficient in CXCR2 or stably expressing CXCR2 crossing inflamed endothelial monolayers under shear flow. The two dHL-60 cells were perfused over monolayers of confluent HDMVECs which had been stimulated with IL-β for 3 hrs to induce E-selectin, integrin ligands and multiple CXCR2 and CCR2 chemokines. (B) Intracellular FACS staining of lamins A/C in permeabilized CXCR2 dHL-60 cells stably expressing the pRetroX-PrelaminA-IRES-ZsGreen1 construct (green) or control CXCR2 dHL-60 cells (black). Dashed line depicts cell staining with an isotype matched control mAb. (C-H) FACS analyzed surface staining of CXCR2, the E-selectin carbohydrate ligand

carrying the HECA-452 epitope, and the integrin subunits CD18, CD11a, CD11b and CD29 on sham (black) vs. ZsGreen1-lamin A/C overexpressing (green) dHL-60 cells. Cells were labeled as described in the Materials and Methods section with either PE conjugated anti-human mAbs or with unlabeled primary antibodies followed by a PE or APC conjugated secondary Ab. (I) Migration tracks of control and lamin A overexpressing dHL-60 cells settled on immobilized CXCL1 analyzed with Imaris 9.0.0 software. The migration tracks are plotted with a common origin (central black dot) and the color code depicts the start and end time points of each track. The average total distance mean ± SD travelled by individual granulocyte-like cells within the indicated experimental groups interacting with immobilized CXCL1 is depicted in parenthesis.

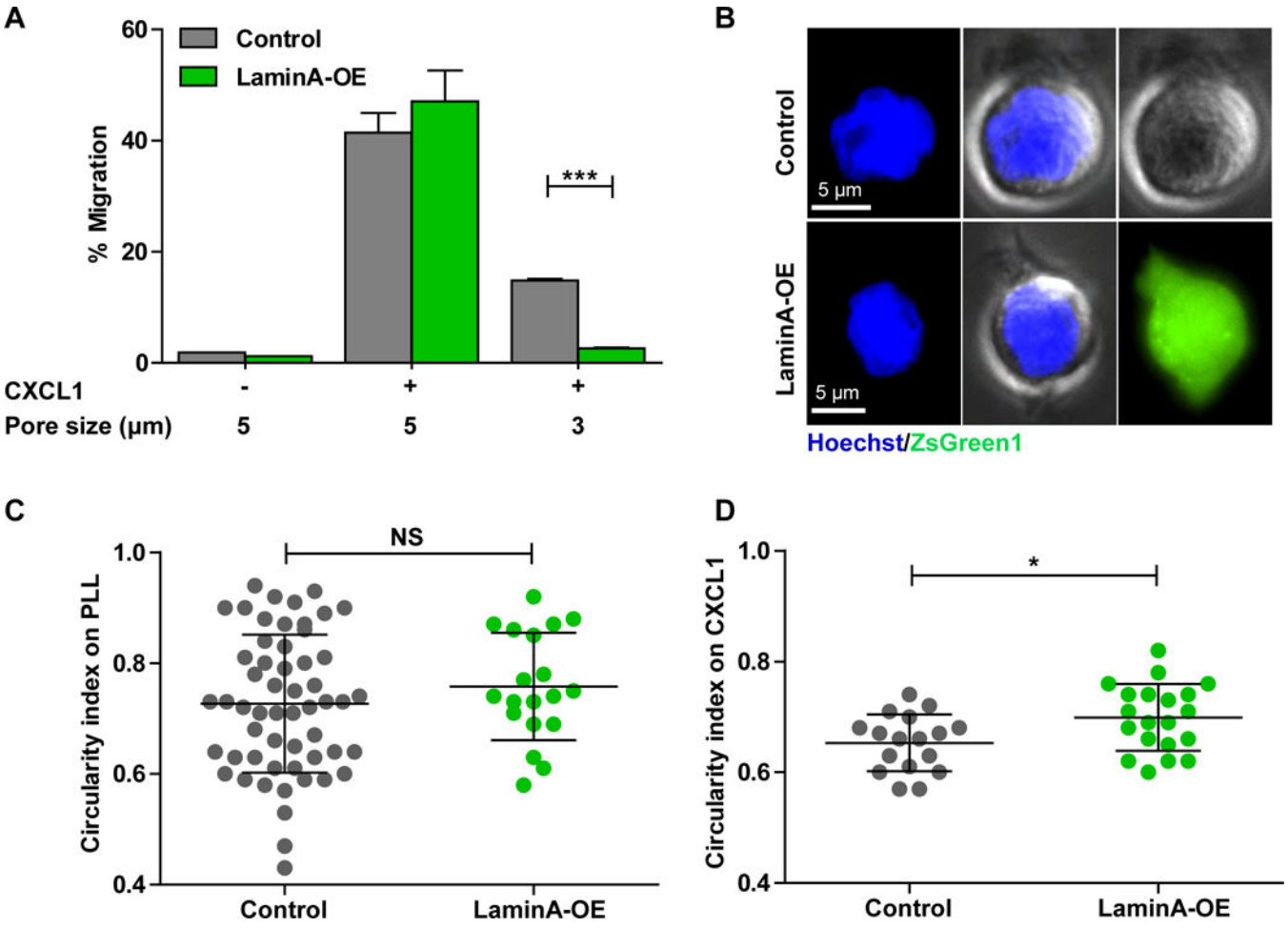

Figure 2. Lamin A overexpression in granulocyte-like HL-60 cells restricts chemotaxis via small rigid pores.

(A) Chemotaxis of control and lamin A overexpressing (LaminA-OE) granulocyte-like CXCR2 expressing dHL-60 cells towards a CXCL1 gradient across transwell membranes with either 3 or 5 micron pore sizes. Cells were collected 30 mins after introduction to the upper wells. The assays were performed in triplicate. Results are representative of two independent experiments. (B) Representative images of Hoechst labeled CXCR2 control (black) and ZsGreen1-lamin A overexpressing (green, LaminA OE cells) dHL-60 cells settled on a PLL coated surface. (C,D) Scatter plots of nuclear circularity index determined for Hoechst labeled control and lamin A overexpressing dHL-60 cells attached to PLL coated surface (C) or immobilized CXCL1 (D). For more details, refer to the Materials and Methods section. The experiments in C and D are each representative of three. Error bars represent mean ± SD. *$p < 0.02$.

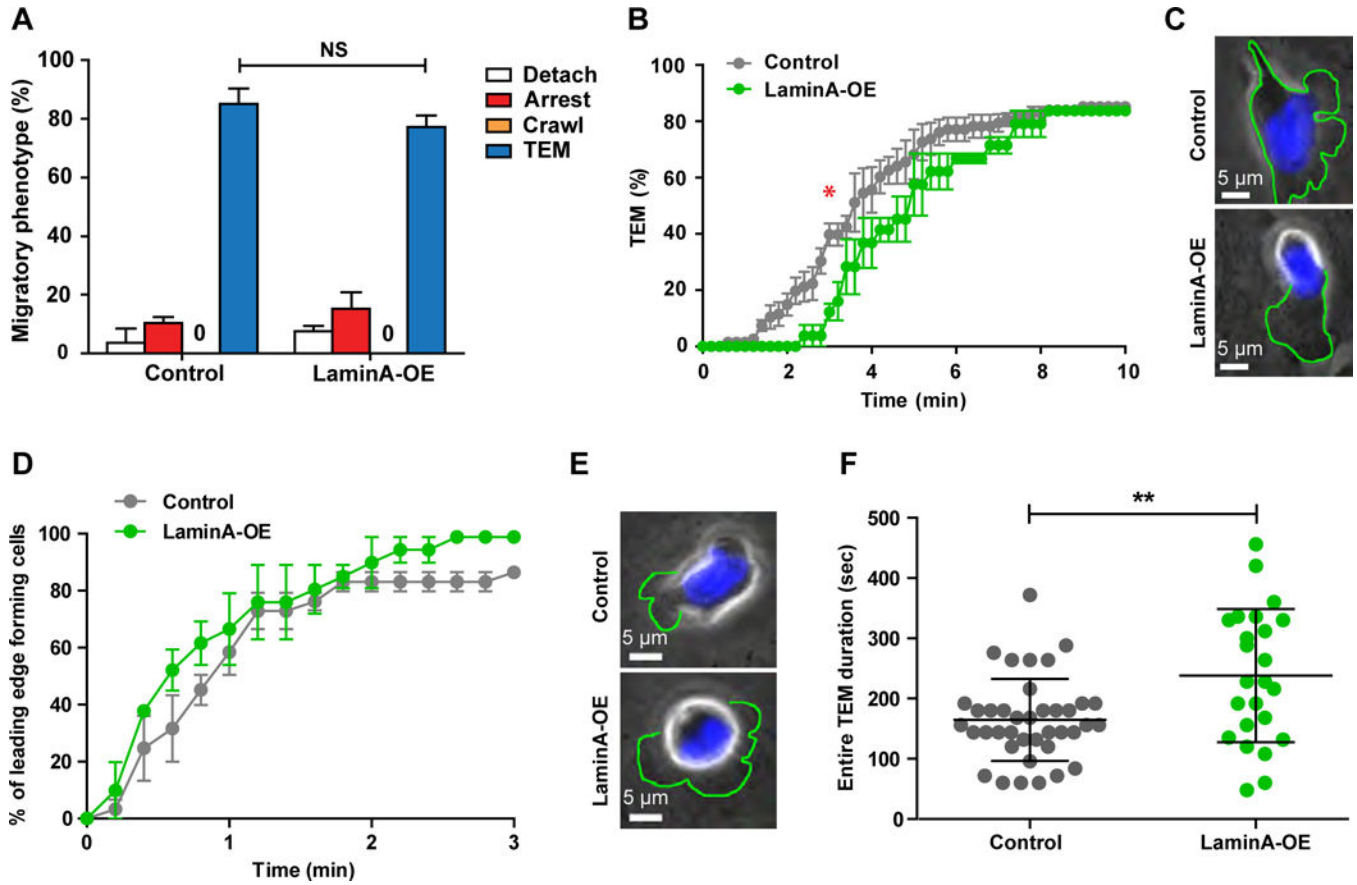

Figure 3. Lamin A overexpression in granulocyte-like HL-60 cells is permissive for TEM across an inflamed IL-1β stimulated HDMVEC monolayer.

(A) Migratory phenotypes of control and lamin A overexpressing (Lamin A-OE) granulocyte-like differentiated CXCR2 expressing HL-60 cells interacting with HDMVECs stimulated for 3 hrs with IL-β under shear flow. Values represent the mean ± SD of three fields in each experimental group. The experiment shown is representative of three. (B) The percentage of granulocyte-like CXCR2 dHL-60 cells that completed transmigration across the inflamed HDMVEC monolayer at the indicated time points following the accumulation phase. Values represent the mean ± SEM of three fields in each experiment. The experiment shown is representative of three. * $p < 0.02$ for t= 3 mins. (C) Images of a representative Hoechst-labeled sham (control) and lamin A overexpressing (LaminA-OE) granulocyte-like dHL-60 cell during paracellular TEM taken 3 mins after the end of the accumulation phase. The green outline depicts the basolateral leading edge of the transmigrating dHL-60 cell. (D) The percentage of dHL-60 cells that projected a protrusive sub-endothelial leading edge underneath the monolayer at the indicated time points prior to nucleus crossing. (E) Images of a representative Hoechst-labeled sham (control) and lamin A overexpressing (LaminA-OE) dHL-60 cell taken 15 sec after the end of the accumulation phase. The green outline depicts the basolateral leading edge generated during the early stage of TEM. (F) TEM kinetics of individual control vs. lamin A overexpressing (LaminA-OE) granulocyte-like CXCR2 dHL-60 cells that crossed the inflamed HDMVEC monolayer measured from the first detectable protrusion of a sub-endothelial leading edge to the final detachment of the

dHL-60 uropod from the apical endothelial aspect. Values were determined in multiple fields taken from three independent experiments. Error bars represent mean ± SD. **p < 0.002.

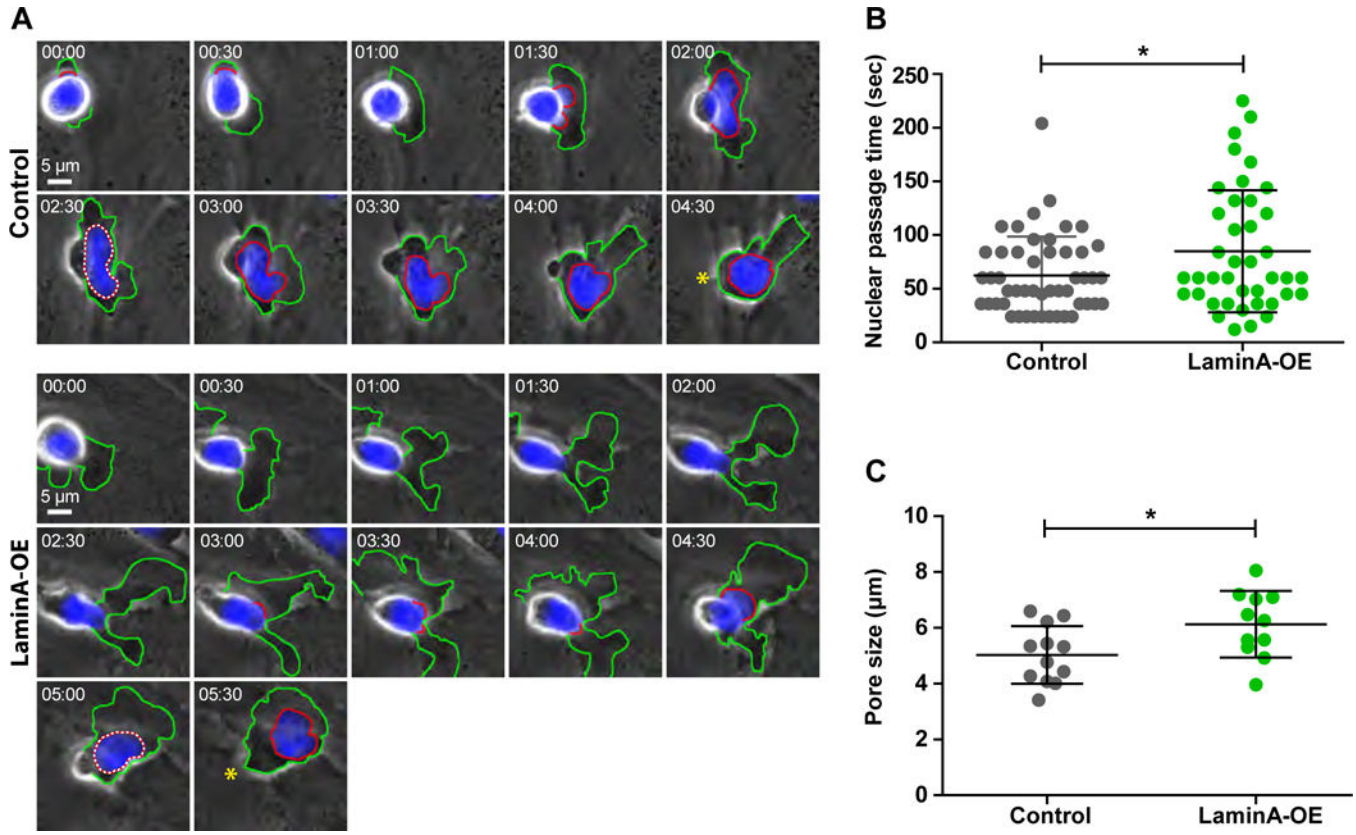

Figure 4. Lamin A overexpressing granulocyte-like dHL-60 cells exhibit slower nuclear squeezing and generate larger endothelial gaps during paracellular TEM.

(A) Images taken from Supplemental Video 1 recording a representative Hoechst-labeled sham (control) and lamin A overexpressing (LaminA-OE) granulocyte-like CXCR2 dHL-60 cell squeezing through paracellular EC junctions. The green outline depicts the basolateral leading edge of the transmigrating dHL-60 cell and the red outline depicts the nuclear lobes inserted underneath the endothelial monolayer. The red circumference of the nucleus is highlighted in white dots at the first time point at which the entire nucleus of each of the transmigrating dHL-60 cells has completed its passage underneath the endothelial monolayer. The yellow asterisks denote the leukocyte uropods at the time of TEM completion. Time intervals are depicted in each image. Scale bar= 5 µm. (B) Nuclear passage duration in individual control and lamin A overexpressing (LaminA-OE) CXCR2 dHL-60 cells transmigrating across inflamed HDMVECs monolayers. Values represent cells from multiple fields taken from three independent experiments. Error bars represent mean ± SD. *$p < 0.03$. (C) The diameter of endothelial gaps generated by crossing granulocyte-like CXCR2 dHL-60 (control vs. LaminA-OE) cells determined as described in Materials and Methods. Values for cells from multiple fields were collected in three independent experiments. Error bars represent the mean ± SD. *$p < 0.03$.

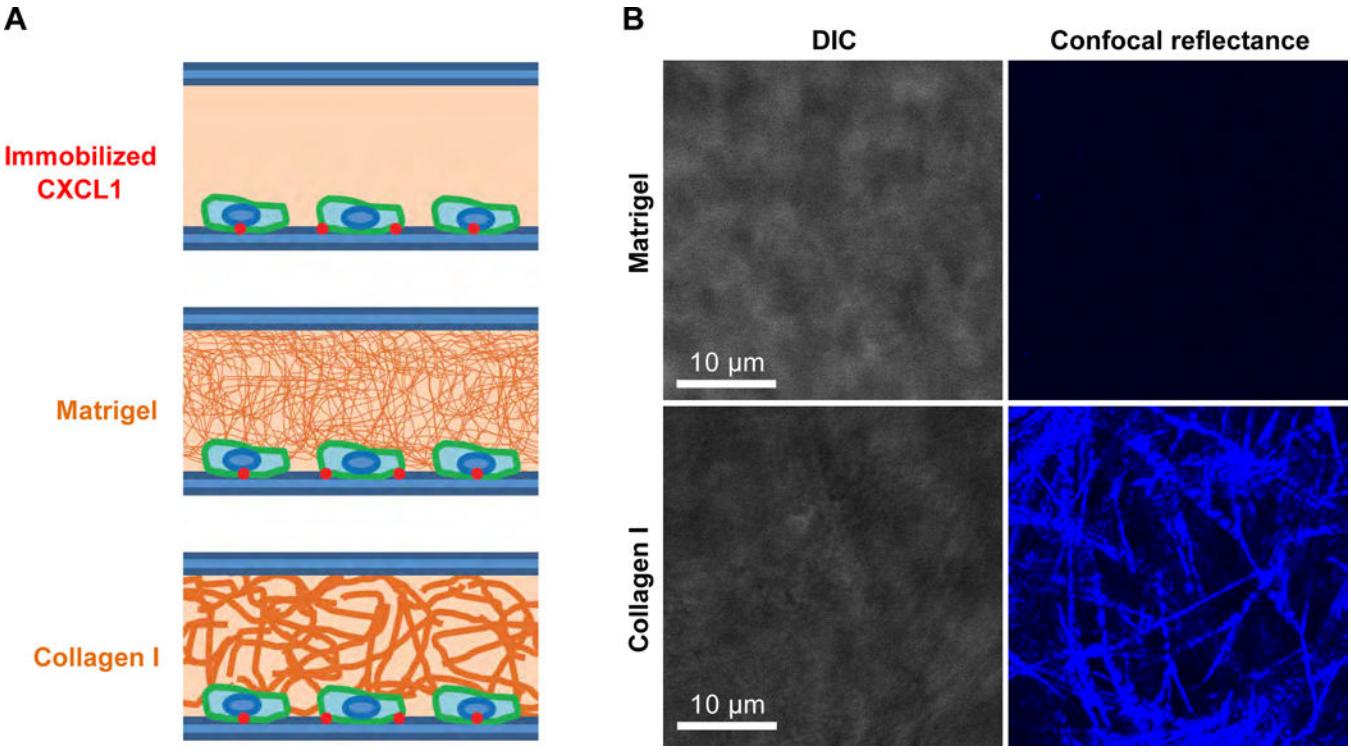

Figure 5. A setup for leukocyte motility on a chemokine-coated surface in the presence of distinct 3D collagenous barriers.

(A) A scheme depicting the experimental model used to assess leukocyte crossing of distinct collagenous barriers. Leukocytes suspended in cold matrigel or collagen I solutions were sedimented for 3 mins and incubated under the distinct collagen solutions for 30 min at 37°C to allow collagen polymerization. Leukocyte motility was recorded for 30 additional minutes. (B) Representative confocal reflectance images of matrigel (50% solution) and collagen 1 matrices (3.2 mg/ml) which underwent polymerization for 30 mins at 37°C. Scale bars= 10μm.

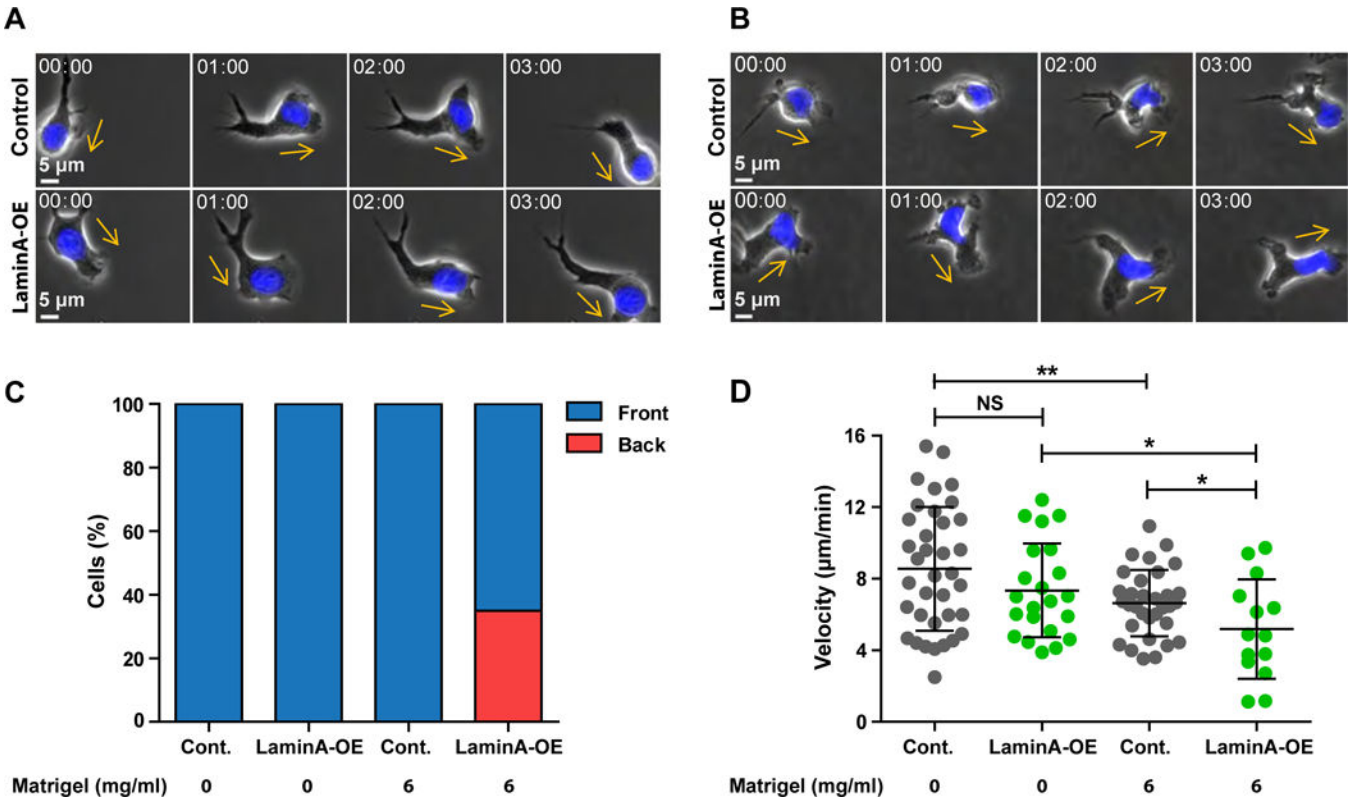

Figure 6. Lamin A overexpression in granulocyte-like cells does not affect their chemokine driven motility through a permissive matrigel barrier.

Images from Supplemental Videos 2 and 3 depicting representative control (A) vs. lamin A overexpressing (LaminA-OE, B) Hoechst-labeled granulocyte-like dHL-60 cells migrating on immobilized CXCL1 either in aqueous medium (left) or when embedded inside a polymerized matrigel matrix (right). Time codes are depicted and scale bars= 5 μm. (C) Nuclear locations in control (Cont.) and lamin A (LaminA-OE) overexpressing Hoechst labeled granulocyte like dHL-60 cells migrating over immobilized CXCL1 either in medium or embedded in polymerized matrigel (50% solution). Results were determined for 40–50 cells from 3 independent experiments. (D) The velocities of individual control (Cont.) and lamin A overexpressing (LaminA-OE) granulocyte-like dHL-60 cells migrating over immobilized CXCL1 alone or when embedded in the polymerized matrigel. Values represent cells from multiple fields taken from three independent experiments. Error bars represent mean ± SD. *$p < 0.05$; **$p < 0.007$.

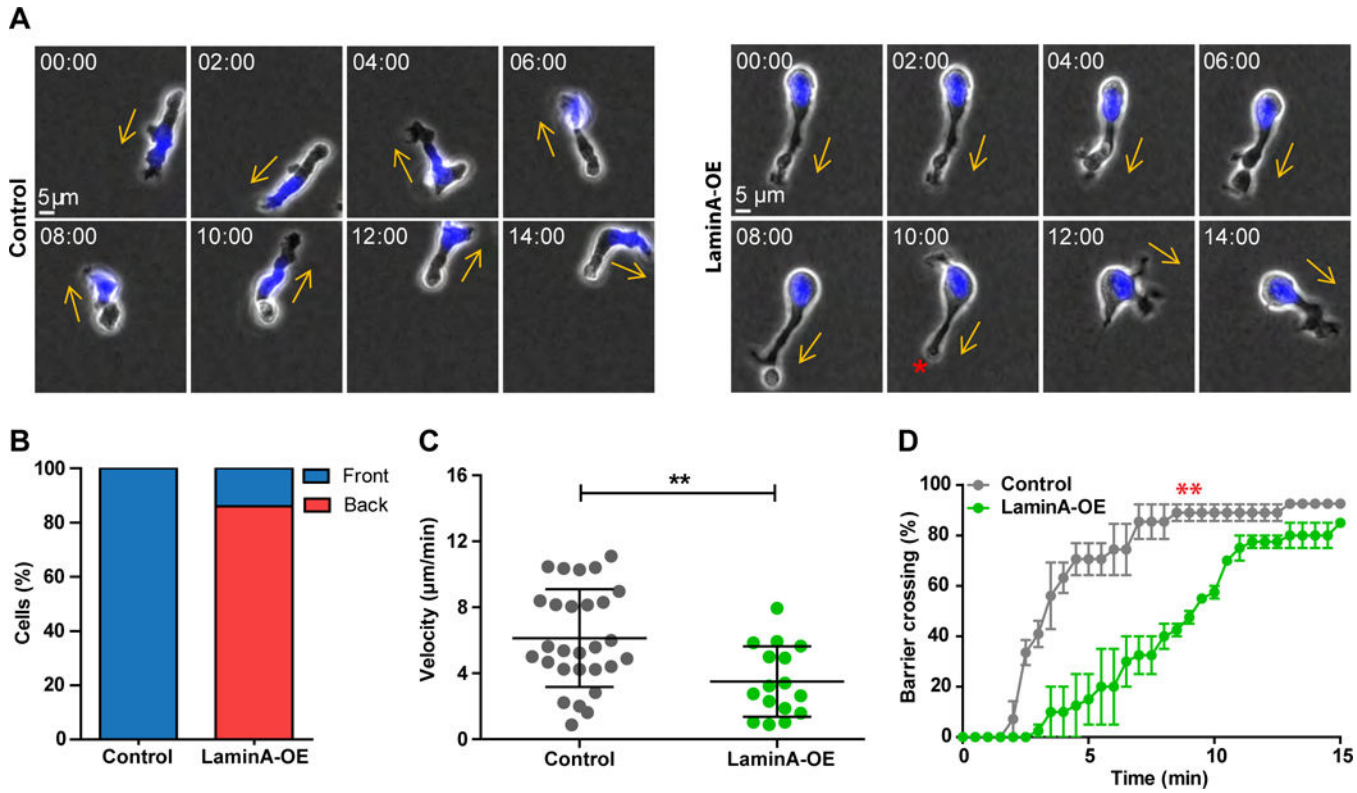

Figure 7. Lamin A overexpression in granulocyte-like cells restricts nucleus squeezing and chemokine driven motility through a dense collagen I barrier.

(A) Images from Supplemental Video 4 depicting representative control vs. lamin A overexpressing (LaminA-OE) Hoechstlabeled granulocyte-like dHL-60 cells migrating on immobilized CXCL1 while being embedded inside a polymerized collagen I matrix (B). Time codes are depicted for each image. Scale bar= 5 µm. Yellow arrows depict the direction of granulocyte motility over the chemokine coated 2D surface. The red asterisk indicates a retracting leading edge. (B) Nuclear locations in control and lamin A overexpressing (LaminA-OE) Hoechst labeled granulocyte like dHL-60 cells migrating over immobilized CXCL1 through the collagen I barrier. Results were determined for 40–50 cells from 3 independent experiments. (C) Scatter plot of velocities of individual control and lamin A/C overexpressing (LaminA-OE) granulocyte-like dHL-60 cells migrating through polymerized collagen I matrices. Values were collected from three independent experiments. Error bars represent mean ± SD. **$p < 0.004$. (D) Kinetics of collagen I barrier crossing of individual control and lamin A overexpressing (LaminA-OE) granulocyte-like dHL-60 cells. The numbers of cells within each experimental group that successfully crossed a 20 µm long barrier of collagen I as a function of time. Values represent the mean ± SEM of three fields. ** $p< 0.01$ for t= 9 mins. The experiment shown is a representative of three.